Charge-storage evolution of TiO_2 ALD-coated AC flexible supercapacitors over long-term cycling

Remuel Isaac M. Vitto[1], Hamed Pourkheirollah[1], Jari Keskinen[1], Paul R. Berger[1,2], Matti Mäntysalo[1]
[1] Faculty of Information Technology and Communication Sciences, Tampere University, Tampere, Finland
[2] Department of Electrical and Computer Engineering, Ohio State University, USA
Email: remuel.vitto@tuni.fi

***Abstract*—Supercapacitors (SCs) are gaining widespread integration into flexible and wearable electronics due to their ability to deliver fast charge transfer at high-power densities. Although incorporation of metal oxides onto carbon-based electrodes presents a promising strategy to enhance the energy density of SCs, their long-term cycling stability remains to be a challenge. In this work, activated carbon (AC) electrodes coated with ultra-thin titanium dioxide (TiO_2) via atomic layer deposition (ALD) were evaluated for long-term cycling (LTC) stability. The TiO_2-coated AC showed excellent capacitance retention of 98% after 10,000 cycles. Trasatti analysis shows a moderate increase in capacitive behavior of TiO_2-coated ACs, indicating a conditioning phase in the initial cycles and a stronger charge transfer mechanism by the end of the LTC due to surface area enlargement and improved pore accessibility from repeated cycling. Furthermore, this increasingly effective energy storage mechanism of AC and TiO_2 results in higher specific capacitance values by 16% initially and up to 32% after the TLC at measurements with constant-voltage hold charge-discharge cycles. Overall, these results highlight an ALD-coated TiO_2 to boost the specific capacitance of AC-based SCs with improved charge-storage mechanism over long-term cycling and maintaining good capacitance retention.**

Keywords—Activated carbon, Titanium dioxide, Atomic layer deposition, Supercapacitors, Printed electronics, Long-term cycling behavior, Capacitance retention

I. Introduction

The recent advancement in flexible electronics continues to become an integral part of modern society, revolutionizing the implementation of technology into our daily lives from embedded textiles to wearable health monitoring sensors. These devices require a reliable and efficient energy storage system that delivers instantaneous energy transfer in a compact and flexible form factor. While conventional lithium-ion batteries possess high-energy density, integration into flexible electronics remains challenging due to safety concerns during mechanical deformation, a short cycle life, and slow ion kinetics. Supercapacitors (SCs), on the other hand, have high-power density and rapid charge transfer with long cycling lifetime [1-3]. However, certain applications of flexible electronics demand high-energy density to extend the operating time between charges and maximize their miniaturization. To overcome the relatively low-energy density of carbon-based SCs, transitional metal oxides are incorporated into the electrode material to combine the intrinsic electric-double layer capacitance (EDLC) of carbon with pseudocapacitance from faradaic redox reactions [4,5].

In our previous study, the specific capacitance of activated carbon (AC) SC electrodes was enhanced by depositing ultra-thin films of titanium dioxide (TiO_2) via atomic layer deposition (ALD) which provides additional surface-redox and intercalation pseudocapacitance [6]. While our previous study presents a promising solution towards enhancing the overall electrochemical performance of AC SCs, its long-term cycling (LTC) stability remains a critical knowledge gap. Especially for applications in flexible and wearable electronics, which must have an energy storage system that operates reliably even after hundreds of thousands of cycles. In general, the poor cycling stability of metal oxides is due to structural degradation from repeated ion intercalation-extraction and surface deterioration from metal-oxygen bonding breakage and dissolution [7]. However, the deposition method of these metals oxides play a key role in their overall cycling stability, wherein ALD creates stronger chemical bonds due to its self-limiting nature which deposits uniform and conformal films compared to other bulk coating methods which are full of defects [7,8]. In addition, the strong and stable porous framework of the AC substrate could prevent material aggregation and structural collapse to improve the electrochemical cycling of TiO_2 [9,10].

In this study, the LTC stability of symmetric SC devices based on TiO_2 ALD-coated AC electrodes was evaluated at 10,000 charge-discharge cycles. The deposition process of TiO_2 varied at 60 and 100 ALD cycles to produce film thicknesses of approximately 2 nm (TiAC60) and 4 nm (TiAC100), along with an uncoated bare AC for comparison. Extensive studies on the SC device capacitance retention through LTC measurements at different applied current densities and on the deposited TiO_2 electrochemical behavior through Trasatti analysis before and after the 10,000 charge-discharge cycles were performed.

II. Experimental Section

The fabrication of the AC electrodes and the ALD process for TiO_2 are based on our previous study which have been reported in detail [6]. A schematic illustration of the experimental procedures is summarized in Fig. 1.

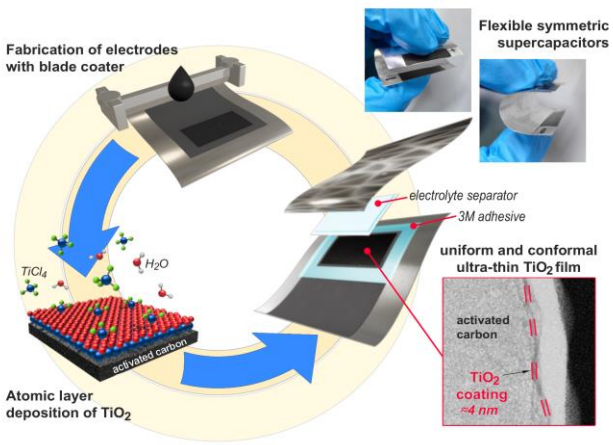

Fig. 1. Schematic illustration of the electrode fabrication, ALD of TiO_2, and assembly of symmetric SCs based on TiO_2 ALD-coated AC electrodes.

A. Electrode Fabrication

The AC ink was composed of 90 wt% Kuraray YP-80F AC as the active material and 10 wt% mixture of (styrene-butadiene rubber, SBR, carboxymethyl cellulose, CMC, and Triton X-100) as the binder material. An mtv-messtechnik doctor blade coater was subsequently used on a graphite ink (Acheson EDAG PF-407C) and on the prepared AC ink to print the current collector and electrode layers onto a 50 µm aluminum/polyethylene terephthalate (Al/PET) substrate.

B. Atomic layer deposition

The ALD process of TiO_2 was done on a Beneq TFS200 system directly onto the fabricated AC electrodes. The precursors used are titanium tetrachloride ($TiCl_4$, Volatec Ltd.) as the titanium-source and deionized water (H_2O) as the oxygen-source. In general, the chemical reactions between the precursors and AC surface are as follows [6]:

$$(A)\quad TiOH\ (s) + TiCl_4\ (g) \rightarrow TiO\text{-}TiCl_3\ (s) + HCl\ (g) \quad (1)$$

$$(B)\quad TiCl\ (s) + H_2O\ (g) \rightarrow Ti\text{-}OH\ (s) + HCl\ (g) \quad (2)$$

where one ALD cycle is composed of the sequential reactions A and B separated by excess precursors purging with nitrogen. The reactions starts at the hydroxyl (–OH) groups on the AC surface and then at the deposited Ti-OH for the succeeding layers. The ALD process was done at a temperature of 120 ˚C with optimized precursor pulsing times of 450 ms for $TiCl_4$ and 300 ms for H_2O to achieve self-limiting growth rate of around 0.4 to 0.6 Å/cycle [6].

C. Electrochemical measurements

The fabricated bare and TiO_2-coated AC electrodes were assembled into symmetrical SC devices using a 3M 468 MP adhesive and a 40 µm Dynacap GT 0.45/40 cellulose electrolyte separator, soaked in a 5:1 mass ratio of water and NaCl (99.5%, Sigma-Aldrich). The LTC behavior was assessed using galvanostatic charge-discharge (GCD) cycles using a high and low current densities for 10,000 continuous cycles on a Maccor 4300 workstation. The charge-discharge cycles were applied with 10 A/g and 5 A/g, and the capacitance was measured every 1,000th cycle at 1 A/g and 0.1 A/g for the high and low current density, respectively. The cyclic voltammetry (CV) measurements were performed at varying scan rates from 1 mV/s to 50 mV/s using a Zahner Zennium potentiostat.

The potential range of the GCD and CV measurements were kept constant at 0.0 to 1.2 V since the electrochemical stability of NaCl electrolytes is typically limited to only around 1.2 to 1.5 V. In our previous study [6], the equivalent series resistance increases significantly when the potential reaches 1.4V due to electrolyte decomposition. The specific capacitance ($C_{specific}$) was determined using comprehensive GCD measurements in accordance with the IEC 62,391-1 industrial standard [11]. This protocol involves four charge–discharge cycles at applied currents of 1, 3, and 10 mA, where the fourth cycle held is held at 1.2 V for 30 min. The $C_{specific}$ values were calculated using the equations:

$$\text{for GCD,} \qquad C_{specific} = I{\cdot}\Delta t \,/\, m{\cdot}\Delta V \quad (3)$$

$$\text{for CV,} \qquad C_{specific} = CV_{area} \,/\, 2{\cdot}m{\cdot}v{\cdot}\Delta V \quad (4)$$

where I is the applied current, Δt is the discharge time, m is the mass of both electrodes, ΔV is the potential range, CV_{area} is the total area of the CV curve, and v is the scan rate.

III. Results and Discussion

A. Long-term cycling behavior

The calculated $C_{specific}$ values before the LTC and capacitance retention values after 10,000 cycles at low and high current are presented in Table I and Fig. 2, respectively.

TABLE I. SPECIFIC CAPACITANCE VALUES

Current	Bare AC	TiAC60	TiAC100
at 1.0 A/g	22 F/g	25 F/g	24 F/g
at 0.1 A/g	29 F/g	34 F/g	35 F/g

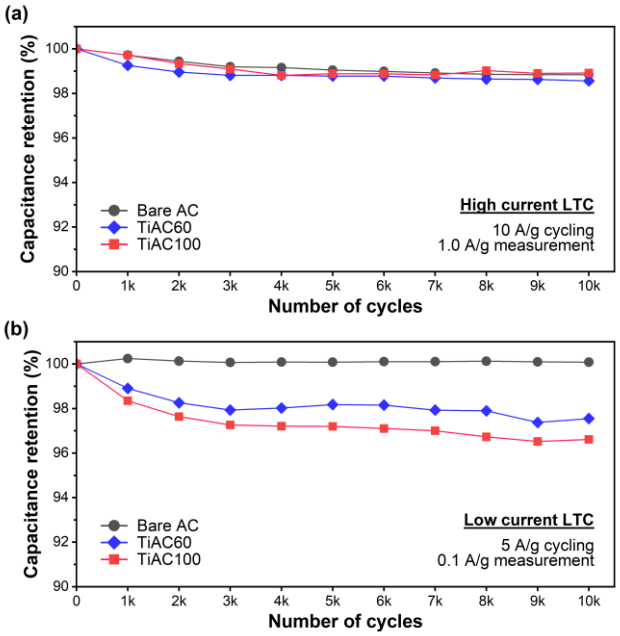

Fig. 2. Capacitance retention of bare AC, TiAC60, and TiAC100 at (a) high and (b) low current density over long-term cycling stability at 10,000 cycles.

In high current density LTC test, both the bare AC and TiO_2-coated ACs displayed excellent cycling stability with a capacitance retention of 99% after 10,000 cycles. Whereas in low current density LTC test, slightly lower capacitance retention was observed at 98% for TiAC60 and 97% for TiAC100 while the bare AC had no measurable capacitance loss. Better cycling stability was observed at high current because it primarily involves surface-situated reactions which have minimal stress on the electrode structure. On the other hand, low current density involves slow ion insertion-extraction that risks surface/structural degradations. Nevertheless, both the TiAC60 and TiAC100 showed excellent cycling stability compared to a similar study done on ALD-coated TiO_2 on AC-based SCs which had 91% capacitance retention after 10,000 cycles [12] and to that of TiO_2 nanotube arrays SCs with a capacitance retention of 83.8% after 5,000 cycles [13]. The remarkable cycling stability exhibited by the TiO_2-coated ACs is probably a result of the combined strong chemical bonds created by the ALD and the structurally stable AC framework [7-10].

B. Varying scan rate

To investigate the degradation and the changes in the charge-storage mechanisms of the TiO_2-coated ACs after the 10,000 cycles, CV measurements were employed at slow and fast scan rates as shown in fig. 3.

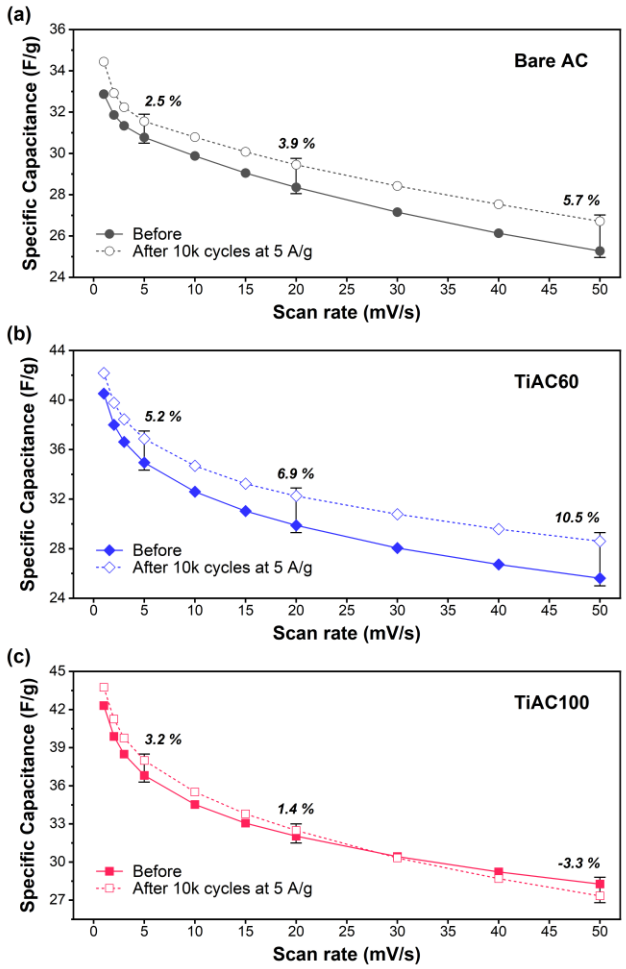

Fig. 3. Specific capacitance values of (a) bare AC, (b) TiAC60, and (c) TiAC100 at varying scan rates before and after the low current density LTC.

The bare AC and TiAC60 had higher $C_{specific}$ after the LTC test, especially at high scan rates. Indicating a charge transfer kinetics that improves overtime until reaching peak efficiency and degrades eventually. For the bare AC, the initial cycles can act as a conditioning phase for the EDLC mechanism. In which the surface area of AC increases from volume expansion after LTC [14], improving the accessibility of electrolyte ions on the micropores and increasing its capacitance. While in the case of TiAC60, similar conditioning phase occurs except it also gives way to the surface-redox pseudocapacitance given by the equation:

$$TiO_2 + Na^+ + e^- \leftrightarrow Na\ TiO_2 \quad (5)$$

This also explains why the increase in $C_{specific}$ after LTC test was higher in TiAC60 compared to bare AC because it is a combination of the overall capacitance from the optimized EDLC and surface-redox. However, slightly lower $C_{specific}$ were observed for TiAC100 at high scan rates. In our previous study [6], the TiAC100 has a film thickness that results in pore blocking which reduces the capacitance at high scan rates. Thus, even though the conditioning phase could also take place in TiAC100, the slight capacitance increase is countered by the lower number of micropores.

C. *Trasatti analysis*

The Trasatti's method was utilized to determine the total capacitance of an electrode and estimate the fast surface-situated capacitive contributions from EDLC and surface-redox and the slow diffusive contributions from ion intercalation/extraction [15,16]. The percentage contributions are calculated using the following equations:

$$Q_T = Q_C + Q_D \quad (6)$$

$$Q_V = Q_C + \alpha v^{-1/2} \quad (7)$$

$$1/Q_V = 1/Q_T + \alpha v^{1/2} \quad (8)$$

where Q_T is the total stored charge, Q_C is the capacitive charge, Q_D is the diffusive charge, Q_v is the total voltammetric charge measured from the CV measurements, v is the scan rate, and α is the resulting slope from the linear fit of the data points from 1 to 5 mV/s in the Q_V versus $v^{-1/2}$ and $1/Q_V$ versus $v^{1/2}$ plot. The resulting percentage of capacitive contributions from the overall capacitance for bare AC, TiAC60, and TiAC100 before and after LTC at low current density are shown in Fig. 4. The highest capacitive charge at 82% was calculated from the bare AC since its charge-storage mechanism is purely EDLC. While the capacitive contribution decreases to 66% for TiAC60 and 33% for TiAC100 due to the additional diffusive contributions from the TiO_2. Most notably, a slight increase by 3% in the capacitive contribution after LTC was observed for TiAC60. Indicating a larger surface area for fast charge transfers and further supports the explanation of volume expansion and better pore accessibility that occurs during the conditioning phase. Furthermore, the low capacitive contribution of TiAC100 denotes a small surface area with majority of charge transfers relying on slow ion intercalations. This also explains the initially low $C_{specific}$ of TiAC100 at fast cycling measurements with high applied current as shown in Table 1.

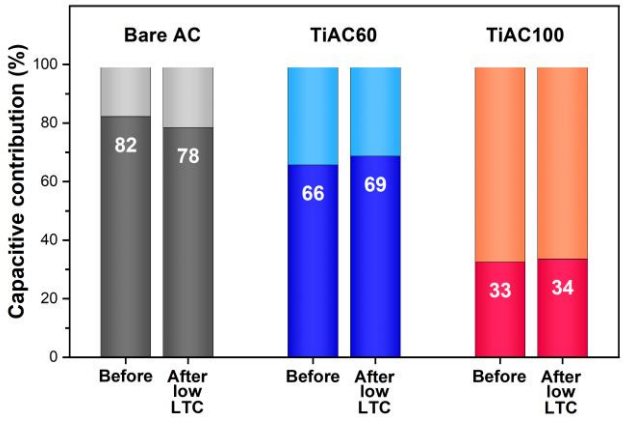

Fig. 4. Estimation of the capacitance percentage from capacitive behavior of the bare AC, TiAC60, and TiAC100 before and after LTC at low current

D. *Specific capacitance values*

The electrochemical behavior before and after the LTC measurements were assessed through comprehensive GCD charge-discharge cycles based on an international standard for evaluating SC performance [11]. The calculated $C_{specific}$ for bare AC, TiAC60, TiAC100 are shown in Fig. 5, wherein the values of before LTC are presented as the average of four samples with standard deviation error bars. In contrast to the CV analysis, the bare AC SCs showed lower $C_{specific}$ values after the low and high current LTC compared to the average $C_{specific}$ before LTC. However, these values fall within the standard deviation error, such that their similar values still indicate good cycling stability.

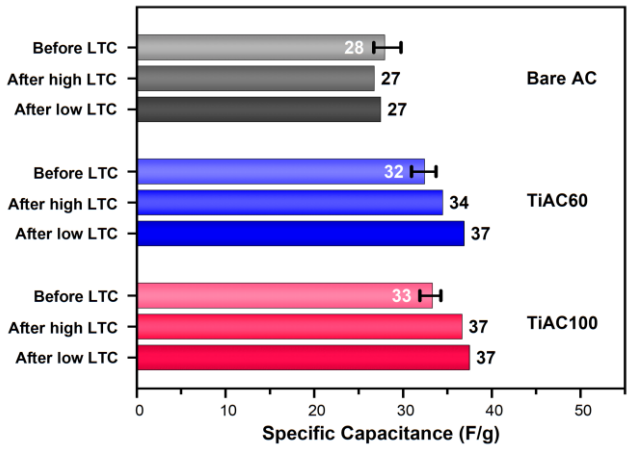

Fig. 5. Calculated specific capacitance values from the IEC 62,391-1 industrial standard GCD measurements of bare AC, TiAC60, and TiAC100 before and after LTC.

Interestingly, both TiO_2-coated AC SCs showed a 13% increase in $C_{specific}$ after the low current LTC compared to the average $C_{specific}$ before LTC. Due to the constant voltage hold at 1.2 V step of the GCD measurement, the electrolyte ions have sufficient time to migrate into the deepest micropores and exhibit higher charge transfer. This method provides a detailed calculation of the capacitance from both surface-situated reactions at the outer and inner pores, but also from the slow diffusion-limited ion intercalations that are otherwise excluded in high scan rate CV measurements. Combining the initial electrochemical performance increase from the TiO_2 coating and the charge transfer improvement, TiAC60 and TiAC100 shows a 32% increase in $C_{specific}$ compared to the bare AC.

IV. Conclusion

This work presents a TiO_2 ALD-coated AC electrode towards high-energy density flexible SCs with a $C_{specific}$ of 34 F/g and excellent capacitance retention of 98% after 10,000 cycles. Demonstrating an effective method of depositing metal oxides via ALD to enhance AC electrochemical performance while maintaining good cycling stability over LTC. Moreover, this work presents new insights into the evolving charge-storage mechanisms of ALD-coated TiO_2 on an AC framework under repeated cycling. In particular, the volume expansion and improved pore accessibility of the electrodes results in higher capacitance through increasing the active sites for EDLC and surface-redox reactions. Overall, the TiO_2-coated AC SC device shows great potential in the application of flexible and wearable electronics as an energy storage system with a reliable cycling lifespan. Future efforts may focus on examining the surface properties of the TiO_2-coated AC electrode before and after LTC, including morphological characterizations, functional group analysis, and surface area and pore volume evaluations.

Acknowledgment

This project, funded by the European Commission's Horizon Europe programme, is part of the Graphene Flagship initiative which works to advance technologies that rely on graphene and other 2D materials. Part of the research uses Research Council of Finland Research Infrastructure 'Printed Intelligence Infrastructure' (PII-FIRI, Grant Number 358618).

References

[1] Shalini, S., Naveen, T. B., Durgalakshmi, D., Balakumar, S., & Rakkesh, R. A. (2024). Progress in flexible supercapacitors for wearable electronics using graphene-based organic frameworks. Journal of Energy Storage, 86, 111260. https://doi.org/10.1016/j.est.2024.111260.

[2] Zhou, X., Zheng, X., Dong, X., Wang, X., Jiang, Y., Li, G., Li, L., Yuan, N., & Ding, J. (2025). Recent advances in wearable fiber-shaped supercapacitors: Materials, design, and applications. Energy Materials, 5(5). https://doi.org/10.20517/energymater.2024.126.

[3] Kumar, N., Lee, S.Y., & Park, S.J. (2026). Bridging EDLC and pseudocapacitive mechanisms through materials design: Recent advances in supercapacitor electrodes. Current Opinion in Solid State and Materials Science, 41, 101251. https://doi.org/10.1016/j.cossms.2025.101251.

[4] Xiong, C., & Su, Y. (2024). Recent progress of transition metal‐based oxide composite electrode materials in supercapacitor. Advanced Sustainable Systems, 9(1). https://doi.org/10.1002/adsu.202400578.

[5] Askari, M. B., & Salarizadeh, P. (2026). A review on activated carbon's role in next-generation supercapacitors. Carbon Trends, 23, 100612. https://doi.org/10.1016/j.cartre.2026.100612.

[6] Vitto, R. I., Pourkheirollah, H., Keskinen, J., Vindt, S., Cook, A., Grīnberga, L., Ignatāne, L., Kučinskis, G., Volperts, A., Tewari, A., Lupo, D., Berger, P. R., & Mäntysalo, M. (2026). Interfacial engineering of conformal titanium oxide nanofilms on porous carbon supercapacitor electrodes via atomic layer deposition. Journal of Power Sources, 662, 238691. https://doi.org/10.1016/j.jpowsour.2025.238691.

[7] Cao, Y., He, Y., Gang, H., Wu, B., Yan, L., Wei, D., & Wang, H. (2023). Stability Study of transition metal oxide electrode materials. Journal of Power Sources, 560, 232710. https://doi.org/10.1016/j.jpowsour.2023.232710.

[8] Feng, J., Xiong, S., & Wang, Y. (2019). Atomic layer deposition of tio2 on carbon-nanotube membranes for enhanced capacitive deionization. Separation and Purification Technology, 213, 70–77. https://doi.org/10.1016/j.seppur.2018.12.026.

[9] Wang, S., Wang, S., Wang, G., Che, X., Li, D., Li, C., & Qiu, J. (2020). Ion removal performance and enhanced cyclic stability of SNO2/CNT composite electrode in Hybrid Capacitive Deionization. Materials Today Communications, 23, 100904. https://doi.org/10.1016/j.mtcomm.2020.100904.

[10] Li, Z., Wang, C., Chen, X., Wang, X., Li, X., Yamauchi, Y., Xu, X., Wang, J., Lin, C., Luo, D., Wang, X., & Zhao, X. S. (2020). Moox nanoparticles anchored on N-doped porous carbon as Li-ion battery electrode. Chemical Engineering Journal, 381, 122588. https://doi.org/10.1016/j.cej.2019.122588.

[11] B.B. Standard, Fixed electric double layer capacitors for use in electronic equipment. Part I: generic specification, BS EN. (1) (2006) 62391.

[12] Bai, Y., Li, N., Yang, C., Wu, X., Yang, H., Chen, W., Li, H., Zhao, B., Wang, P.-F., & Han, X. (2021). Realizing high-voltage and Ultralong-life supercapacitors by a Universal Interfacial Engineering Strategy. Journal of Power Sources, 510, 230406. https://doi.org/10.1016/j.jpowsour.2021.230406

[13] Clement Raj, C., Jothi Prakash, C. G., & Prasanth, R. (2021). Engineering electrode/electrolyte interfacial properties of nanotube arrays for high-capacitance supercapacitors. Journal of Materials Science: Materials in Electronics, 32(8), 11119–11128. https://doi.org/10.1007/s10854-021-05778-w

[14] Yang, S., Zhao, F., Li, X., Cao, B., Mo, Y., Chen, D., & Chen, Y. (2019). Electrode structural changes and their effects on capacitance performance during preparation and charge-discharge processes. Journal of Energy Storage, 24, 100799. https://doi.org/10.1016/j.est.2019.100799

[15] Harish, S., & Sathyakam, P. U. (2025). Dunn's method for distinguishing charge storage mechanisms in supercapacitors: A status quo review. Journal of Electronic Materials, 54(12), 10858–10872. https://doi.org/10.1007/s11664-025-12481-7

[16] Allagui, A., & Elwakil, A. S. (2023). Tikhonov regularization for the deconvolution of capacitance from the voltage–charge response of electrochemical capacitors. Electrochimica Acta, 459, 142527. https://doi.org/10.1016/j.electacta.2023.142527